Journal of Hazardous Materials 187 (2011) 274–282

Contents lists available at ScienceDirect

Journal of Hazardous Materials

journal homepage: www.elsevier.com/locate/jhazmat

Removal of water-soluble acid dyes from water environment using a novel magnetic molecularly imprinted polymer

Xubiao Luo[a,b], Youcai Zhan[a,b], Yining Huang[a,b], Lixia Yang[a,b], Xinman Tu[a,b], Shenglian Luo[a,b,*]

[a] College of Environmental and Chemical Engineering, Nanchang Hangkong University, Nanchang 330063, PR China
[b] Key Laboratory of Jiangxi Province for Ecological Diagnosis-Remediation and Pollution Control, Nanchang 330063, PR China

ARTICLE INFO

Article history:
Received 1 October 2010
Received in revised form
27 December 2010
Accepted 5 January 2011
Available online 12 January 2011

Keywords:
1-(α-Methyl acrylate)-3-methylimidazolium bromide
Water-soluble acid dyes
Magnetic molecularly imprinted polymer
Removal

ABSTRACT

Novel magnetic and hydrophilic molecularly imprinted polymers (mag-MIPs) were prepared by an inverse emulsion–suspension polymerization to remove water-soluble acid dyes from contaminated water with 1-(α-methyl acrylate)-3-methylimidazolium bromide (1-MA-3MI-Br) being utilized as a new functional monomer. The thermal stability, chemical structure and magnetic property of the 1-MA-3MI-Br-mag-MIPs were characterized by the thermal-gravimetric analyzer (TGA), Fourier transform infrared spectrometer (FT-IR) and vibrating sample magnetometer (VSM), respectively. Moreover, effect of concentration and pH value of water-soluble acid dye solutions was optimized. Compared with the methyl acrylic acid and 4-vinylpyridine modified mag-MIPs, the 1-MA-3MI-Br-mag-MIPs showed enhanced removal efficiency. Kinetic studies depicted that the adsorption process on 1-MA-3MI-Br-mag-MIPs followed pseudo-second-order rate mechanism. Investigation results of 5 times removal–regeneration cycles by employing the 1-MA-3MI-Br-mag-MIPs showed that the resulting material was with high stability.

1. Introduction

Dyes are widely used in many industries such as textiles, rubber, paper, plastics and so on. About over 7×10^5 t 10,000 different commercial dyes and pigments are produced annually all around the world. It has been estimated that about 10–15% of these dyes are lost during the dyeing process and released with the effluent [1]. The presence of these dyes in water, even at very low concentrations, is highly visible and undesirable. Many dyes are difficult to degrade due to their complex structures, and some of them are toxic, mutagenic and carcinogenic [2]. Therefore, removing dyes from wastewater of industrial effluents before discharging them into the environment is extremely important.

A lot of techniques such as oxidation [3–5], biological treatment [6–9], or applying activated carbon [10–16], ion-exchange [17–20], and chitosan [21,22], have been developed to remove the water-soluble acid dyes. At present, the most common treatment for effective dyestuff removal is adsorption. Malik [23] and Attia et al. [24] reported that the activated carbon exhibited high removal efficiency for acid blue, acid red and acid yellow dyes from aqueous solution due to its chemical and mechanical stability, high adsorption capacity and high degree of surface reactivity. Ion-exchange is another effective method for dyes removal. Karcher et al. [17,18] proved that weakly and strongly basic anion exchange resins of commercial names Lewatit S6328A and Lewatit MP-62 exhibited good sorption and reusability characteristics for reactive red and reactive black dyes contained in wastewater from textile industry. Wawrzkiewicz and Hubicki [25] also evaluated the strongly basic anion exchange resin (Purolite A-520E) and activated carbon (Purolite AC-20G) for the treatment of Acid Blue 29 solutions. In addition, Wong et al. [26] successfully applied chitosan to eliminate acid dyes such as acid green, acid orange, and Shen et al. [27] developed an efficient combination of chitosan adsorption and catalytic oxidation method for removing acid red.

Although satisfied results have been achieved by the above methods, most of them are high-cost, low reuse, tedious post-processing and with secondary pollution. In addition, all of these absorbents are applied for non-specific absorption in industry, exhibiting poor selectivity. Therefore, a selective absorption method is required to separate the toxic or precious water-soluble acid dyes from mixture. Selective separation of water-soluble acid dyes will facilitate the environment protection and the reuse of precious water-soluble acid dyes.

Molecular imprinted polymers (MIPs) are a type of synthesized material with specific recognition ability for the template molecules. In comparison with the common absorbents such as active carbon, the MIPs are with higher reusability, selectivity and lower consumption. To date, MIPs have been widely used in

* Corresponding author at: College of Environmental and Chemical Engineering, Nanchang Hangkong University, Fenghe South Street 696, Nanchang 330063, PR China. Tel.: +86 791 3953372; fax: +86 791 395373.
E-mail addresses: luoxubiao@126.com (X. Luo), sllou@hnu.cn (S. Luo).

0304-3894/$ – see front matter © 2011 Elsevier B.V. All rights reserved.
doi:10.1016/j.jhazmat.2011.01.009

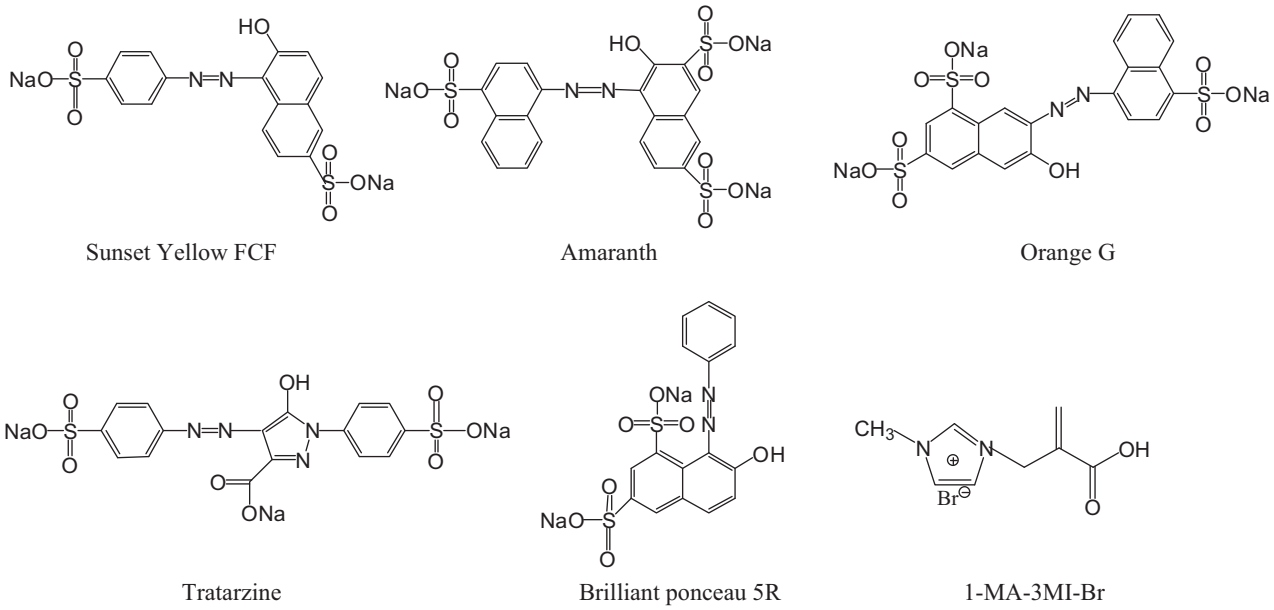

Fig. 1. Molecular structures of the five water-soluble acid dyes and 1-MA-3-MI-Br.

many areas such as solid-phase extraction [28], chromatograph separation [29], membrane separations [30], sensors [31], and catalysts [32]. The molecular imprinting technique also has applied for the determination and removal of pesticides and endocrine-disrupting compounds from waste and drinking water [33–37]. These molecularly imprinted polymers were generally prepared with methacrylic acid (MAA), 4-vinylpyridine (4-VP), acrylamide (AM) as functional monomers [38–40]. However, on account of these functional monomers are poor hydrophilic capacity, the synthesized MIPs showed poor imprinted efficiency in water media. Furthermore, application of these MIPs is a very complicated procedure which needs filtration or centrifugation. Consequently, it is desirous to develop hydrophilic MIPs which can remove acid dyes from wastewater effectively, and can be easily collected.

The mag-MIPs can make separation process simple and fast, because it can be easily collected by an external magnetic field without additional centrifugation or filtration. Recently, mag-MIPs have been prepared and applied in pollution removal. For example, microwave heating was used in preparing mag-MIP beads for removing trace triazines analysis in complicated samples [41]. Bovine serum albumin surface-imprinted sub-micrometer particles with magnetic susceptibilities were prepared by using miniemulsion polymerization method [42]. Core–shell magnetic molecular imprinted polymers were prepared by the surface RAFT polymerization for the fast and selective removal of endocrine disrupting chemicals from aqueous solution [37]. To the best of our knowledge, there is no report on water-compatible mag-MIPs by using inverse emulsion–suspension polymerization.

In this work, new magnetic and hydrophilic molecularly imprinted polymers were prepared by inverse emulsion–suspension polymerization and applied for removing water-soluble acid dyes from wastewater. The resulting functional material is easily operated due to the magnetism. Furthermore, high removal efficiency and selectivity in adsorbing acid dyes can be achieved by applying the 1-MA-3MI-Br-mag-MIPs.

2. Experimental

2.1. Chemicals

Trimethylolpropane trimethacrylate (TRIM) were obtained from Chinese Qianjin Chemistry Reagent Factory (Tianjin, China). Hydroxyethyl Cellulose (HEC), 4-vinyl pyridine (4-VP), meth acrylic acid (MAA), and 2,2-azobisisobutyronitrile (AIBN) were purchased from Beijing Chemical Reagent Factory (Beijing, China). Amaranth, brilliant ponceau 5R, orange G, sunset yellow FCF, and tratarzine (shown in Fig. 1) were supplied by Pure Crystal Shanghai Reagent Co., Ltd. (Shanghai, China). Span80, methanol, acetic acid, ammonia solution (28%) and ammonium acetate were obtained from Guangzhou Chemical Reagent Factory (Guangzhou, China). HPLC-grade methanol was purchased from Dima Technology (Richmond Hill, USA). Ethylene glycols (PEG 6000) were obtained from Xilong Chemical Plant (Shantou, China). Ferric chloride ($FeCl_3{\cdot}6H_2O$) and ferrous sulfate ($FeSO_4{\cdot}7H_2O$) were supplied from Shenyang Chemical Industry Corporation (Shenyang, China). Strongly anion exchange solid phase extraction was obtained from Agela Technologies' Corporation (Tianjin, China). 1-(α-Methyl acrylate)-3-methylimidazolium bromide (1-MA-3MI-Br) was synthesized in our laboratory (shown in Fig. 1). The structure was confirmed by 1H NMR and IR analysis. Water was purified through a Milli-Q water system (Bedford, USA).

2.2. Instruments and analytical methods

Aliquots of 10 μL were analyzed on an HP 1100 HPLC system (Agilent Technologies, Palo Alto, CA, USA), which consisted of a HPLC pump operating at a flow rate of 1.0 mL/min, and DAD monitoring the effluent at 254 nm for all compounds. The analytical column was a 250 mm × 4.6 mm, 5 μm C_{18} column (Agilent, USA). The mobile phase was methanol:20 mM ammonium acetate buffer solution (20:80, V/V). IR spectra were recorded with a Shimadzu IR-prespige-21 FT-IR spectrometer as KBr pellets (Tokyo, Japan). The pH of each solution was measured by using microprocessor based pH meter, model number HI 8424 (M/s Henna Instruments, Italy).

The size and morphology of 1-MA-3MI-Br-mag-MIPs was investigated by a scanning electron microscope (Philips XL-20®, FEI Company, Hillsboro, OR, USA). The surface area of the synthesized polymer was determined by an F-Sorb 3400 automatic surface area analyzer (Gold APP Instrument, Beijing, China) in a BET nitrogen adsorption and desorption mode after appropriate degassing and drying of the sample. Thermal stability of the particles was measured using a thermogravimetric analyzer (TGA-50H, Shimadzu, Japan). Measurements were conducted by scanning from room

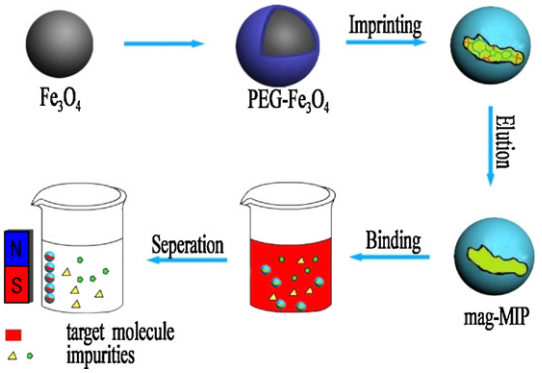

Scheme 1. Synthesis route of water-compatible mag-MIPs and their application for removal of water-soluble acid dyes with the help of an external magnetic field.

temperature to 700 °C at a rate of 10 °C/min. Magnetic properties were analyzed using a vibrating sample magnetometer (VSM, LDJ9600, USA).

2.3. Sample preparation

Wastewater was collected from a nearby factory in Nanchang, and the river water sample came from Gan Jiang River in Nanchang city, China. Samples were filtered through a 0.45 μm nylon membrane (Gelman Sciences, Ann Arbor, USA) before using.

2.4. Preparation of Mag-MIPs

The preparation of water-compatible mag-MIPs is schematically illustrated in Scheme 1. It involves the synthesis of PEG–Fe_3O_4 magnetic fluid, the surface of PEG–Fe_3O_4 being packed by MIPs, final elution of water-soluble acid dyes and generation of the recognition site.

2.4.1. Preparation of Fe_3O_4

Firstly, 0.50 mol/L $FeCl_2$ solution, 0.25 mol/L $FeCl_3$ solution, and 1 mol/L NaOH solution were prepared, then 10 g PEG was added and completely dissolved in 50 mL 60 °C water. Secondly, 10 mL $FeCl_2$ solution and 40 mL $FeCl_3$ solution were added in the PEG solution and reacted for 4 h at 60 °C followed by the drop wise addition of 40 mL NaOH solution. The final brown suspension was placed for 24 h quiescence, and the supernatant was discarded. The residues were Fe_3O_4 magnetic fluid.

2.4.2. Preparation of inverse emulsion

2 mL toluene with 0.1 g AIBN was mixed in 50 mL beaker. When AIBN was dissolved, 10 mL TRIM and a drop of Span 80 were added in the mixture and stirred to be uniform. Then 10 mL Fe_3O_4 magnetic fluid was added in the mixture. The mixture was stirred for 5 min, and then the mixture was submerged in the ultrasonic bath (Kedao Company, Shanghai, China) for 5-min irradiation. Finally, the inverse emulsion can be obtained.

2.4.3. Mag-MIPs and magnetic non-imprinted polymers (mag-NIPs) were prepared via inverse emulsion–suspension polymerization

Firstly, 80 mL water was poured into 250 mL three-neck flask. After that, 0.15 g HEC was added and stirred until it dissolved. Secondly, 1 mmol tratarzine and 4 mmol 1-MA-3MI-Br were added into 50 mL water. After it dissolved, it was prepolymerized for 30 min. The mixture was added into the three-necked flask, and followed by the addition of inverse emulsion. Thirdly, the reaction mixture was heated and purged by N_2 to remove the oxygen. The reaction temperature was preserved at 70 °C for 12 h. After the reaction completed, the resulting mag-MIPs with uneluted molecule were filtered by 120 mesh sieve and washed by methanol and 60 °C water. Finally, the products were eluted by methanol/ammonia solution (9/1, v/v) for 24 h. The mag-NIPs were prepared by the same manner in the absence of template molecules.

Except the different functional monomers, the preparation methods of MAA-mag-MIPs and 4-VP-mag-MIPs were as identical as that of 1-MA-3-MI-Br-mag-MIPs.

2.5. Adsorption studies

1.0 g 1-MA-3-MI-Br-mag-MIPs were dispersed in 50 mL 100 mg/L acid dyes aqueous solution to investigate the effect of pH value on the removal of water-soluble acid dyes from aqueous solution. The initial pH value of the solutions was adjusted from 1 to 11 by using 0.5 mol/L HCl and 0.5 mol/L NaOH. The absorption mixtures were shook at room temperature for 2 h. Adsorption experiments for water-soluble acid dyes were conducted by a batch method. The amounts of water-soluble acid dyes absorbed by the polymers were evaluated by the residual concentrations of it in the magnetic separated aqueous solutions, which were determined by an HPLC with a DAD detector.

In order to evaluate the effect of concentration on the removal efficiency with mag-MIPs, different concentrations 50, 100, 150, 200 mg/L of water-soluble acid dyes solutions were investigated. After absorption, these mag-MIPs were separated under an external magnetic field, and the supernatant was collected and analyzed by HPLC.

In order to investigate the regeneration of 1-MA-3MI-Br-mag-MIPs, adsorbed 1-MA-3MI-Br-mag-MIPs were dipped in methanol/ammonia solution (9/1, v/v) for 24 h. After that, the 1-MA-3MI-Br-mag-MIPs were separated and washed with distilled water and then dried in a vacuum for the reuse.

Removal efficiencies of different kinds of water sources using different sorbents were investigated. The performance of the 1-MA-3MI-Br-mag-MIPs, MAA-mag-MIPs and 4-VP-mag-MIPs in removing water-soluble acid dyes was compared. After absorption, these mag-MIPs were separated under an external magnetic field, and the supernatant was collected and analyzed by HPLC.

2.6. 1-MA-3MI-Br-mag-MIPs and SAX-SPE conditions

2.6.1. SAX-SPE conditions

The SAX-SPE columns were conditioned with 10 mL methanol and 10 mL acid water (pH = 2). 2 mL 10 mg/L spiked wastewater (pH = 2) were loaded in SPE columns at the flow rate of 1 mL/min. Then the cartridge was washed by 10 mL methanol. Finally, the SPE cartridge was eluted with 2 mL methanol/hydrochloric acid solution (8:2, v/v) at the flow rate of 1 mL/min.

2.6.2. 1-MA-3MI-Br-mag-MIPs conditions

(a) *Conditions*: 1.0 g of 1-MA-3MI-Br-mag-MIPs was added into a conical flask. The polymers were conditioned in sequence with 10.0 mL methanol and 10.0 mL water. The mag-MIPs were separated by an external magnet and the supernatant was discarded.
(b) *Extraction*: 20 mL of 10 mg/L of water-soluble acid dyes spiked wastewater was added into the conical flask, the mixture was stirred for 15 min. The supernatant was discarded.
(c) *Washing*: The polymers capturing water-soluble acid dyes were washed with 10 mL methanol. The supernatant was discarded.
(d) *Elution*: The water-soluble acid dyes were eluted from the 1-MA-3-MI-Br-mag-MIPs by 6 mL methanol:ammonia solution (9:1, v/v) three times.

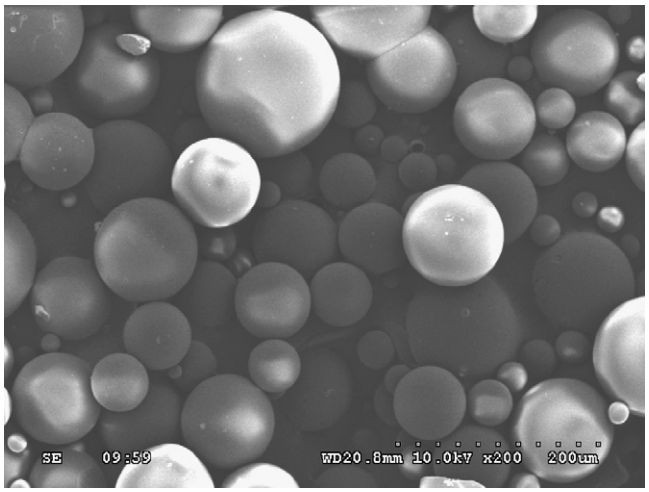

Fig. 2. SEM images of 1-MA-3MI-Br-mag-MIPs.

The elution was combined and evaporated to dryness under nitrogen gas at 60 °C, and the residue was reconstituted with 0.3 mL of water for HPLC analysis.

3. Results and discussion

3.1. The characterization of 1-MA-3-MI-Br-mag-MIPs

3.1.1. Morphology and surface area of 1-MA-3-MI-Br-mag-MIPs

The morphology of 1-MA-3MI-Br-mag-MIPs was observed by SEM. As is shown in Fig. 2, the well shaped particles with diameter distribution from 20 to 100 μm are achieved. Majority of the particles are spherical. Spherical molecular imprinting polymers have large surface area, indicating that large number of effective imprinting sites could exist in the surface to rebind the template molecules in aqueous media.

The surfaces areas of 1-MA-3MI-Br-mag-MIPs and 1-MA-3MI-Br-mag-NIPs were determined by nitrogen sorption measurements. The surface areas of 1-MA-3MI-Br-mag-NIPs and 1-MA-3MI-Br-mag-MIPs were 12.5 and 11.2 m^2/g, respectively. There is no obvious difference between the surface areas of 1-MA-3MI-Br-mag-MIPs and 1-MA-3MI-Br-mag-NIPs. Therefore, the difference of adsorption efficiencies between the 1-MA-3MI-Br-mag-MIPs and 1-MA-3MI-Br-mag-NIPs in the subsequent study could not be attributed to the morphological difference of 1-MA-3MI-Br-mag-MIPs and 1-MA-3MI-Br-mag-NIPs, but to the imprinting effect.

3.1.2. FT-IR analysis of 1-MA-3-MI-Br-mag-MIPs

To ascertain whether imprinted polymers have successfully packed on the surface of Fe_3O_4, FT-IR was employed to characterize Fe_3O_4. In Fig. 3(a), the absorption band at 571 cm^{-1} corresponded to the Fe–O bond for Fe_3O_4 particles. As shown in Fig. 3(b), the peaks at 1340 cm^{-1} and 1470 cm^{-1}, 2890 cm^{-1}, 3430 cm^{-1} are attributed to the flexure vibration of the C–H, the stretching vibration of C–H and the stretching vibration of O–H bond, respectively, indicating that the PEG are successfully packed on Fe_3O_4 surface. In Fig. 3(c), the characteristic peaks assigned to 1270 cm^{-1} (C–O), 1389 cm^{-1} and 1480 cm^{-1} (C–H), 1730 cm^{-1} (C=O), 2970 cm^{-1}(C–H), 3450 cm^{-1} (–OH) reveal that the PEG–Fe_3O_4 has converted to 1-MA-3-MI-Br-mag-MIPs.

3.1.3. VSM of 1-MA-3-MI-Br-mag-MIPs

VSM analysis was applied to study the magnetic property of PEG–Fe_3O_4 and magnetic 1-MA-3-MI-Br-mag-MIPs. The samples were dried at 300 K for the analysis. The magnetic hysteresis loops illustrated in Fig. 4 show that the materials magnetically respond to an external magnetic field. A saturation magnetization of 31.43 emu/g is obtained on the PEG–Fe_3O_4 magnetite which decreases to 4.06 emu/g due to the shielding of the polymeric coating resulting from the modification process. However, the 1-MA-3-MI-Br-mag-MIPs with declined saturation magnetization value also possess enough magnetic response to meet the need of magnetic separation.

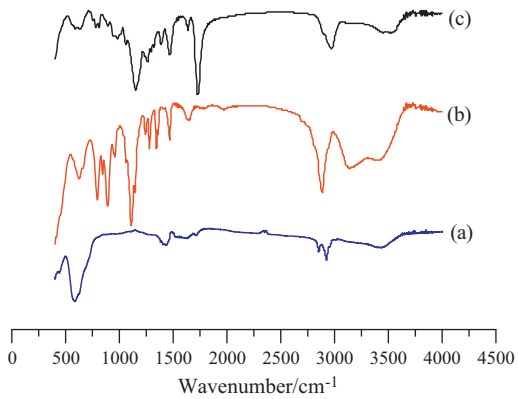

Fig. 3. Infrared spectra of Fe_3O_4 (a), PEG–Fe_3O_4 (b), and 1-MA-3-MI-Br-mag-MIPs (c).

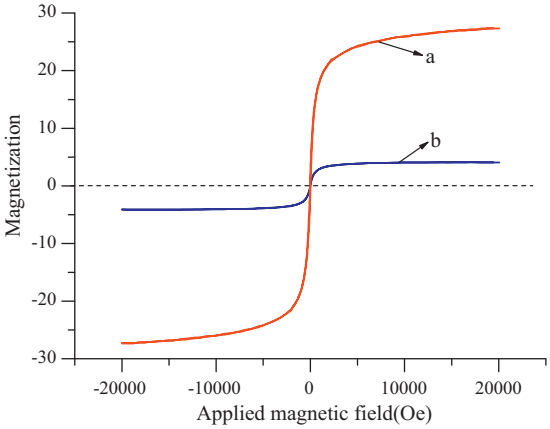

Fig. 4. VSM magnetization curves of PEG–Fe_3O_4 and 1-MA-3-MI-Br-mag-MIPs (a: PEG–Fe_3O_4, *S*, saturation magnetization is 31.43 emu/g; b: 1-MA-3-MI-Br-mag-MIPs, *S*, saturation magnetization is 4.06 emu/g).

3.1.4. Thermogravimetric analysis of 1-MA-3-MI-Br-mag-MIPs

As shown in Fig. 5, the TG curve of 1-MA-3-MI-Br-mag-MIPs is composed of three stage of mass change from room temperature (RT) to 700 °C. The first stage occurred from RT to 298 °C, the decrease of weight was 5.70%, which may due to the dehydration of the water residues in the 1-MA-3-MI-Br-mag-MIPs. The high weight decrease in the second stage from 298 °C to 435 °C was 80.10%, and the value is 3.26% in the third stage from 435 °C to 700 °C, which is caused by the loss of imprinted polymer layer. The total mass loss is calculated to be 89.06 wt%. The residue can be attributed to the more thermally resistant Fe_3O_4 magnetite, giving a magnetite encapsulation efficiency of 10.94 wt%. The achieved encapsulation efficiency was considerably high and satisfactory. The result is consistent with the observation in the VSM analysis.

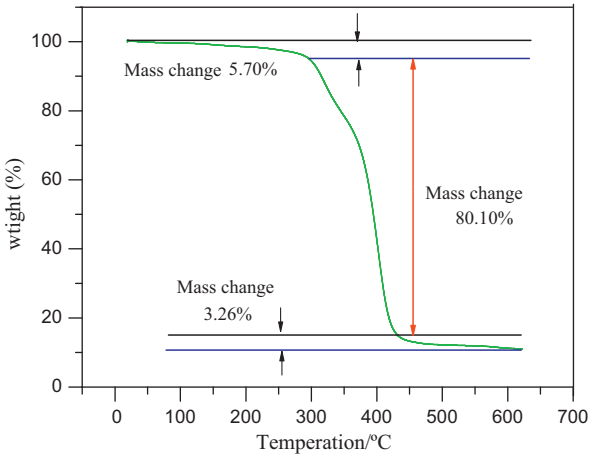

Fig. 5. TGA graph of 1-MA-3-MI-Br-mag-MIPs.

3.2. Adsorption isotherms

The absorption isotherm experiments for 1-MA-3MI-Br-mag-MIPs and 1-MA-3MI-Br-mag-NIPs were carried out in the tratarzine concentration range of 0.05–0.60 g/L (Fig. 6). The amount of absorbed tratarzine per unit mass of the polymer increases along with the increasing of tratarzine initial concentrations, while the binding amount of tratarzine on the imprinted polymer is much higher than that on the non-imprinted polymer in the whole concentration range, displaying the molecular imprinting effect.

The Freundlich isotherm model is generally used to account for heterogeneous binding sites in imprinted polymers [43–45].

$$\text{Freundlich model}: \log Q = \log \alpha + m \log C \quad (1)$$

where Q (mg/g) is the amount of adsorbed analyte per unit of polymer mass, and C (g/L) is the concentration of the analyte in solution at equilibrium. α and m are the two Freundlich constants. The parameter m is the heterogeneity index, with values from 0 to 1, indicating homogeneity of the sites.

Table 1 summarizes the fitting coefficients of the 1-MA-3MI-Br-mag-MIPs and 1-MA-3MI-Br-mag-NIPs, the apparent number of binding sites ($N_{K_{min}} - N_{K_{max}}$), and the apparent average association constant ($\bar{K}_{K_{min}-K_{max}}$), calculated using Eqs. (2) and (3).

$$N_{K_{min}-K_{max}} = \alpha(1-m^2)\ (K_{min}^{-m} - K_{max}^{-m}) \quad (2)$$

$$\bar{K}_{K_{min}-K_{max}} = \left(\frac{m}{m-1}\right)\left(\frac{K_{min}^{1-m} - K_{min}^{1-m}}{K_{min}^{-m} - K_{max}^{-m}}\right) \quad (3)$$

The values for these parameters can be calculated for any range of binding affinities within the limits of the K_{min} and K_{max} being equal to the reciprocal corresponding concentrations $K_{min} = 1/C_{max}$ and $K_{max} = 1/C_{min}$. The calculated results are listed in Table 1.

The data also show that $N_{K_{min}} - N_{K_{max}}$ of tratarzine in 1-MA-3-MI-Br-mag-MIPs is 3.3 times higher than 1-MA-3-MI-Br-mag-NIPs. This results show that the number of sites with adequate geometry and good accessibility to tratarzine is higher in 1-MA-3-MI-Br-mag-MIPs than that in 1-MA-3-MI-Br-mag-NIPs, demonstrating the imprinting phenomenon.

3.3. Removal efficiency of water-soluble acid dyes using different pH

In the work, pH value of the solution is an important factor in controlling the surface charge of the adsorbent and the degree of ionization of the adsorbent in the solution. Fig. 7 shows that the removal efficiency of the 1-MA-3-MI-Br-mag-MIPs increases with the decreased pH value. The acid dyes can be almost completely adsorbed by 1-MA-3-MI-Br-mag-MIPs in the pH range from 1 to 3. Since hydrogen ions can easily combine with the bromide ion of mag-MIPs in acidic media, the positively charged imidazole ring of mag-MIPs would be in a state of lack of electron. Consequently, electrostatic force can be formed between sulfonate ion of the acid dyes and the positively charged imidazole ring. However, in alkaline condition, the hydroxyl ions abundantly existing in the solution are more negatively charged than sulfonate ions, resulting in poor combining force between the sulfonate ions of the acid dyes and the positively charged imidazole ring. Therefore, increasing initial pH values of solution would result in the decrease in removal efficiency of the 1-MA-3-MI-Br-mag-MIPs.

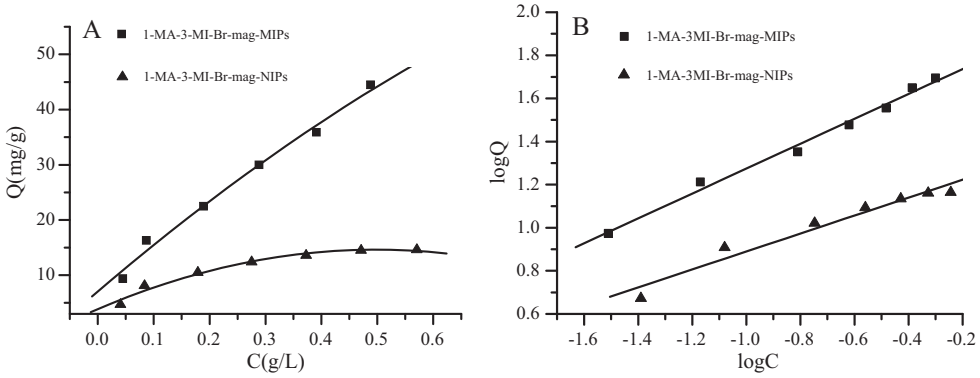

Fig. 6. Adsorption isotherm of tratarzine on 1-MA-3MI-Br-mag-MIPs and 1-MA-3MI-Br-mag-NIPs (A) and fitting to the Freundlich isotherm (B). Conditions: 0.1 g sorbent, 50 mL of tratarzine, shaking time 2 h, temperature 25 °C.

Table 1
Freundlich fitting parameters, weighted average affinity, and number of sites for 1-MA-3-MI-Br-mag-MIPs and 1-MA-3-MI-Br-mag-NIPs.

	m	α	R^2	$N_{K_{min}} - N_{K_{max}}$ (mg/g)[a]	$\bar{K}_{K_{max}-K_{max}}$ (mL/g)[a]
1-MA-3-MI-Br-mag-MIPs	0.58 ± 0.01	72.01 ± 1.7	0.96	25.43 ± 0.60	8.12 ± 0.75
1-MA-3-MI-Br-mag-NIPs	0.42 ± 0.04	20.01 ± 0.9	0.99	8.32 ± 0.69	6.87 ± 0.34

[a] Calculated for a concentration range log K = 1.51–0.24 (g/L).

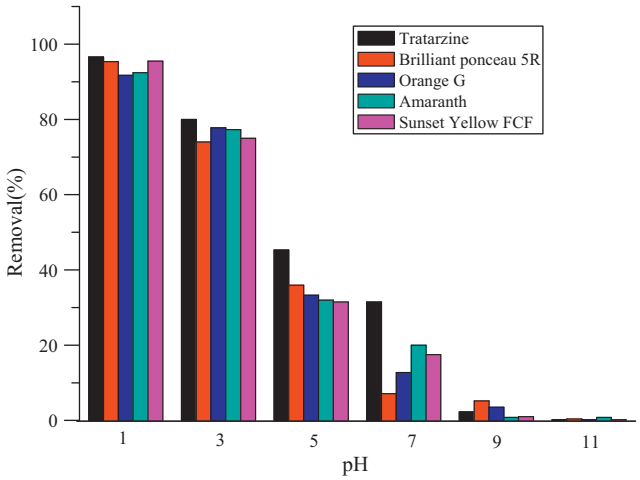

Fig. 7. Removal efficiency of 1-MA-3-MI-Br-mag-MIPs toward water-soluble acid dyes in different pH conditions. Conditions: 1.0 g sorbent, 50 mL of 100 mg/L mixture of water-soluble acid dyes, shaking time 2 h, temperature 25 °C.

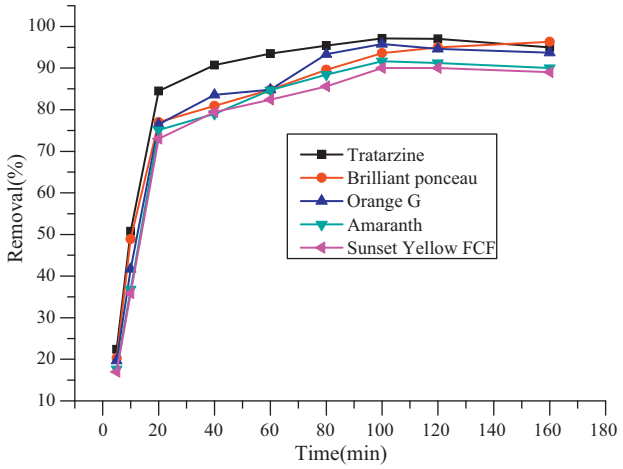

Fig. 9. Removal kinetic curves of 1-MA-3MI-Br-mag-MIPs toward water-soluble acid dyes. Conditions: 1.0 g sorbent, 50 mL of 100 mg/L mixture of water-soluble acid dyes, shaking time 3 h, temperature 25 °C.

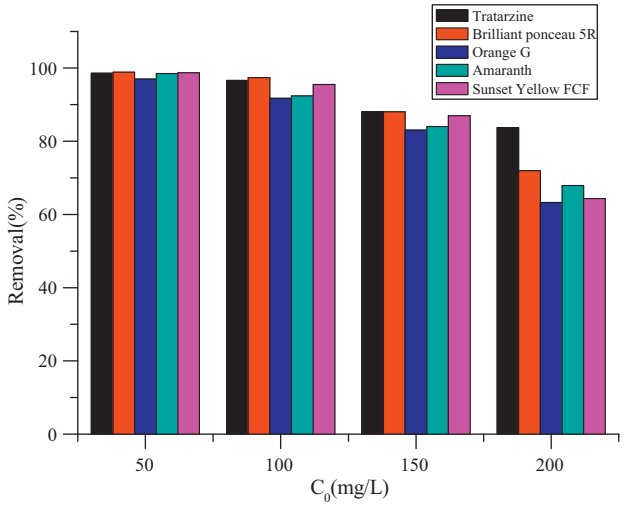

Fig. 8. Removal efficiency of 1-MA-3-MI-Br-mag-MIPs toward water-soluble acid dyes in different concentrations. Conditions: 1.0 g sorbent, 50 mL mixture of water-soluble acid dyes, shaking time 2 h, temperature 25 °C.

3.4. Effects of initial acid dye concentrations on the removal efficiency of 1-MA-3-MI-Br-mag-MIPs

The plots in Fig. 8 show that high removal efficiencies of water-soluble acid dyes are observed at low concentrations such as 50 and 100 mg/L. Removal efficiencies of five kinds of water-soluble acid dyes by applying 1-MA-3-MI-Br-mag-MIPs are almost 100%. The efficiencies decline with the increased acid dye concentrations, which is caused by the limited capability of 1-MA-3-MI-Br-mag-MIPs.

3.5. Removal kinetics of water-soluble acid dyes onto 1-MA-3-MI-Br-mag-MIPs

The removal kinetic curves of the 1-MA-3MI-Br-mag-MIPs in adsorbing acid dyes depicted in Fig. 9 show that the removal process consists of two stage. During the first stage, fast removal rates of the dyes are observed, resulting from the abundant molecule imprinted cavities on the surface of the 1-MA-3MI-Br-mag-MIPs. 20 min later, the removal kinetic curves reach a stable platform, the second stage, suggesting that the adsorption almost has reached the equilibrium. The short time in reaching the adsorption equilibrium indicates that the mag-MIPs are of high absorbability.

The removal kinetic curves of these five kinds of acid dyes fitted the rate Eq. (4) developed by Ho and McKay [46]. The corresponding kinetic parameters are summarized in Table 2. These kinetic data gave a view of the mechanism of 1-MA-3MI-Br-mag-MIPs and potential rate controlling steps.

$$\frac{t}{q_t} = \frac{1}{k_2 q_e^2} + \frac{1}{q_e} t \tag{4}$$

where q_e is the equilibrium amount of water-soluble acid dyes absorbed by the 1-MA-3MI-Br-mag-MIPs. q_t is the absorption amount of 1-MA-3MI-Br-mag-MIPs at any time. k_2 is the second-order rate constant at the equilibrium.

The data exhibit a linear relationship with R all above 0.995. The calculated q_e obtained from the pseudo-second-order model (ranging from 5.00 to 5.18 mg/g) were close to the experimental q_e (ranging from 4.50 to 4.90 mg/g) values for the five water-soluble acid dyes. Above observations show that this model can be applied to predict the adsorption kinetic and the overall rate-constant appears to be controlled by an electrostatic interaction between the sulfonate ion of water-soluble acid dyes and positively charged imidazole ring of mag-MIPs.

Table 2
Kinetic parameters of the second-order rate equation for five water-soluble acid dyes adsorption on 1-MA-3-MI-Br-mag-MIPs.

Acid dyes	Tratarzine	Amaranth	Orange G	Brilliant Ponceau 5R	Sunset Yellow FCF
k_2 (g/mg/min)	0.0216	0.0143	0.0147	0.0140	0.0137
q_e (mg/g)	5.18	5.26	5.22	5.06	5.00
$k_2 q_e^2$ (mg/g/min)	0.573	0.400	0.400	0.358	0.343
R	0.997	0.998	0.996	0.995	0.995

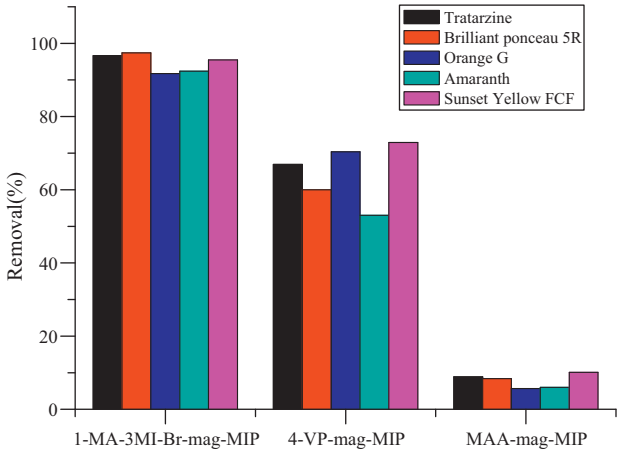

Fig. 10. Removal efficiency of three different sorbents toward water-soluble acid dye. Conditions: 1.0 g sorbent, 50 mL of 100 mg/L mixture of water-soluble acid dyes, shaking time 2 h, temperature 25 °C.

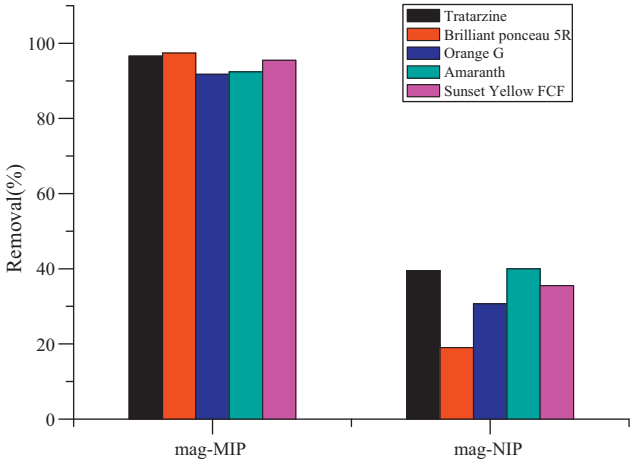

Fig. 11. Removal efficiency of mag-MIPs and mag-NIPs. Conditions: 1.0 g sorbent, 50 mL of 100 mg/L mixture of water-soluble acid dyes, shaking time 2 h, temperature 25 °C.

3.6. Comparison of removal efficiency

3.6.1. Removal efficiency of water-soluble acid dyes using three different sorbents

The absorption investigations toward the water-soluble acid dyes at the optimal condition by applying 1-MA-3MI-Br-mag-MIPs, MAA-mag-MIPs and 4-VP-mag-MIPs were conducted to evaluate the removal efficiencies of these three mag-MIPs. The corresponding data in Fig. 10 show that the efficiency (91.7–97.4%) on 1-MA-3MI-Br-mag-MIPs is much higher than 4-VP-mag-MIPs (53.0–72.9%) and MAA-mag-MIPs (5.7–10.1%). The high removal capacity of 1-MA-3MI-Br-mag-MIPs toward water soluble acid dyes can be attributed to the three interactions, hydrogen bonding, electrostatic, and π–π interactions, between the MIPs and template molecule. Moreover, the removal efficiency of 4-VP-mag-MIPs for water soluble acid dyes was also higher than that of MAA-mag-MIPs. That is because 4-VP-mag-MIPs have hydrogen bonding and electrostatic interaction with template while MAA-mag-MIPs only have hydrogen-bonding action. These results reveal that the above multiple interactions enhance removal ability of 1-MA-3MI-Br-mag-MIPs in adsorbing the target compounds in water environment.

3.6.2. Removal efficiency of 1-MA-3MI-Br-mag-MIPs and 1-MA-3MI-Br-mag-NIPs

Fig. 11 shows that the removal of water-soluble acid dyes by employing 1-MA-3MI-Br-mag-MIPs is more effective than 1-MA-3MI-Br-mag-NIPs. The removal efficiencies on 1-MA-3MI-Br-mag-MIPs in removing the five water-soluble are 95.5%, 92.4%, 91.7%, 97.4%, and 96.6%, respectively. While those on 1-MA-3MI-Br-mag-NIPs are 35.5%, 40.0%, 30.7%, 19.0%, and 39.5%, respectively. The higher absorbability of 1-MA-3MI-Br-mag-MIPs is caused by the abundant imprinted cavities providing the specific absorption for the acid dyes. However, the 1-MA-3MI-Br-mag-NIPs only supply the non-specific absorption, resulting in the poor performance in removing the dyes.

3.6.3. Extraction efficiency of 1-MA-3MI-Br-mag-MIPs and SAX in spiked waste water

In order to compare the extraction performance of the 1-MA-3MI-Br-mag-MIPs and SAX-SPE, a wastewater sample was treated as described in Section 2. Fig. 12 presents the HPLC chromatograms which correspond to the raw wastewater samples (A), spiked wastewater sample (B), spiked wastewater sample after a clean-up by SAX-SPE (C), and spiked wastewater sample after a clean-up by 1-MA-3MI-Br-mag-MIP-SPE (D). The wastewater extracted by 1-MA-3MI-Br-mag-MIPs shows more stable baselines and higher selectivity than that obtained by SAX-SPE. According to the experiment results, the advantages of 1-MA-3MI-Br-mag-MIPs compared with SAX are addressed as below. Firstly, the application of 1-MA-3MI-Br-mag-MIPs can eliminate most interference of complex matrix, which will facilitate the detection and quantification of five kinds of water-soluble acid dyes in this complex matrix. Secondly, the recoveries of five kinds of water-soluble acid dyes on 1-MA-3MI-Br-mag-MIPs (from 91.7% to 97.4%) were higher than that of SAX-SPE (from 71.5% to 91.0%). Moreover, the purities (purity = (the sum of the peak areas of five acid dyes/total peak areas) × 100%) of the recycled five kinds of acid dyes conducted by the 1-MA-3MI-Br-mag-MIPs and SAX-SPE, are 93.2% and 53.4%, respectively. The high purity of the five kinds of acid dyes by 1-MA-3MI-Br-mag-MIPs provides a possibility to recycle the acid dyes from the wastewater

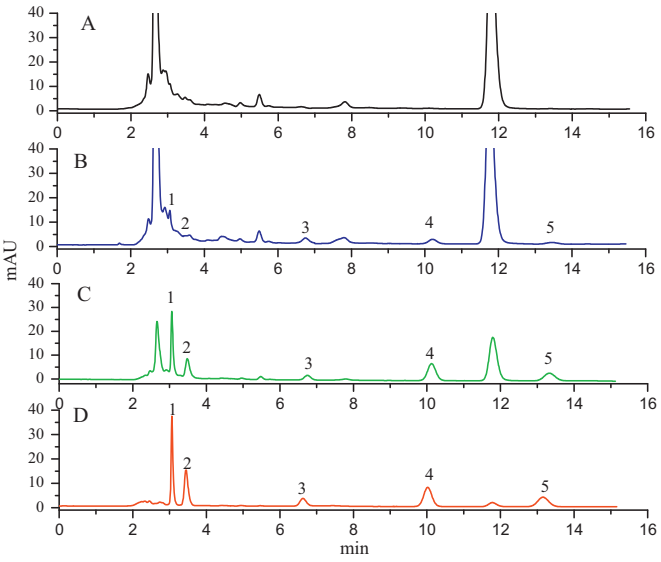

Fig. 12. Chromatograms of five water-soluble acid dyes in different water samples. Raw wastewater sample (A), spiked wastewater sample (B), spiked wastewater sample after a clean-up on SAX-SPE (C), and spiked wastewater sample after a clean-up on 1-MA-3-MI-Br-mag-MIPs (D). Peak 1: tratarzine; Peak 2: amaranth; Peak 3: Orange G; Peak 4: Brilliant ponceau 5R; Peak 5: Sunset Yellow FCF.

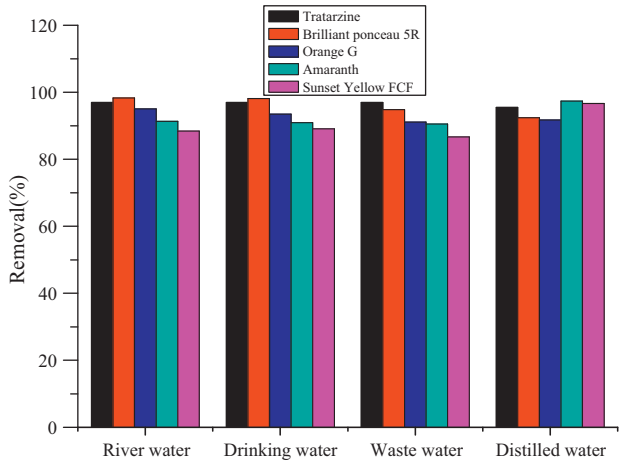

Fig. 13. Removal efficiency of 1-MA-3MI-Br-mag-MIPs toward different kinds of water. Conditions: 1.0 g sorbent, 50 mL of 100 mg/L mixture of water-soluble acid dyes, shaking time 2 h, temperature 25 °C.

efficiently. Furthermore, 1-MA-3MI-Br-mag-MIPs can be easily separated by the external magnetic field, avoiding the complicated process of filling column and pretreatment in traditional SAX-SPE. Consequently, the 1-MA-3MI-Br-mag-MIPs show a promising potential in recycling the acid dyes from wastewater conveniently.

3.6.4. Comparison with other adsorbents

Compared with other adsorbents, the adsorption capacity of 71.12 mg/g obtained on 1-MA-3MI-Br-mag-MIPs is higher than macroporous anion exchanger (acid blue 29, 21.40 mg/g) [25], chitosan (acid red 73, 27.5 mg/g) [27], and strongly basic polystyrene anion exchange resins (tartrazine, 50.00 mg/g) [19]. Although 71.12 mg/g is lower than that 133.30 mg/g obtained on non-living aerobic granular sludge toward acid yellow, 1-MA-3MI-Br-mag-MIPs exhibits much higher selectivity in comparison with the aerobic granular sludge [9]. The above results indicate that 1-MA-3MI-Br-mag-MIPs are reliable and effective adsorbents to remove and utilize acid dyes from wastewater.

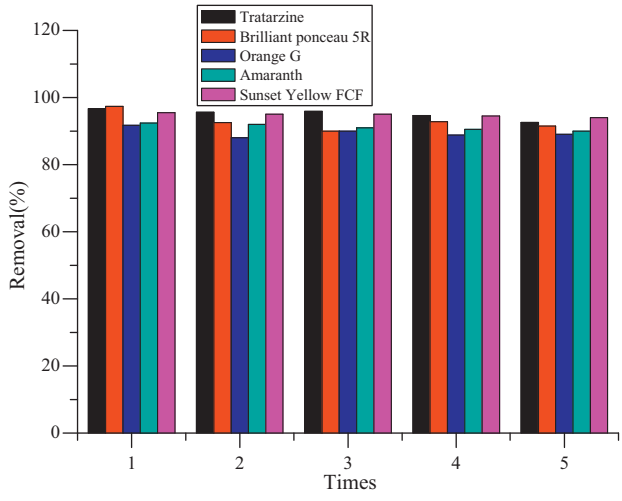

Fig. 14. Stability and potential regeneration of the 1-MA-3-MI-Br-mag-MIPs. Conditions: 1.0 g sorbent, 50 mL of 100 mg/L mixture of water-soluble acid dyes, shaking time 2 h, temperature 25 °C.

3.7. Removal efficiency of environmental water samples using 1-MA-3MI-Br-mag-MIPs

Removal efficiencies of 1-MA-3MI-Br-mag-MIPs in adsorbing the water-soluble acid dyes from different water sources, 50 mL 100 mg/L of spiked waste water, drinking water, river water and distilled water are illustrated in Fig. 13. As the plots shown us, 1-MA-3MI-Br-mag-MIPs exhibit almost 100% removal efficiencies in removing water-soluble acid dyes from the different water sources, suggesting that 1-MA-3MI-Br-mag-MIPs show a strong anti-interference ability in different water environments.

3.8. Regeneration/reuse of 1-MA-3MI-Br-mag-MIPs

The stability and potential regeneration/reuse of the 1-MA-3MI-Br-mag-MIPs were investigated. Removal efficiencies of repeating application of 1-MA-3MI-Br-mag-MIPs are shown in Fig. 14. It is stable for up to five adsorption cycles without obvious decrease in the removal efficiency for water-soluble acid dyes. The experimental results indicate that the 1-MA-3MI-Br-mag-MIPs have excellent reuse/regeneration ability.

4. Conclusions

Our study results demonstrate the several remarkable advantages of the water-compatible 1-MA-3MI-Br-mag-MIPs to remove and recycle the water-soluble acid dyes in water media. First of all, the removal efficiency toward water-soluble acid dyes is very high with all above 95% in distilled water, tap water, river water and wastewater. Moreover, this method realizes an efficient way to recycle the water-soluble acid dyes in water media; and the 1-MA-3MI-Br-mag-MIPs can be reused at least five times without obvious decrease in the removal efficiency. Compared with 4-VP-mag-MIPs and MAA-mag-MIPs, the water-compatible 1-MA-3MI-Br-mag-MIPs show higher removal efficiency and selectivity. In addition, due to the encapsulated Fe_3O_4, the 1-MA-3MI-Br-mag-MIPs can be easily separated by external magnetic field. Consequently, employing 1-MA-3MI-Br-mag-MIPs as absorbents avoids the complicated process of filling column and pretreatment in traditional SAX-SPE, which is a reliable, effective and convenient method to remove and recycle water-soluble acid dyes in aqueous media.

Acknowledgements

This work was financially supported by a grant from the National Science Fund for Distinguished Young Scholars (50725825), the National Natural Science Foundation of China (50978132), the Natural Science Foundation of Jiangxi Province (2009GQH0083), and the Science and Technology Support Program of Jiangxi Province (2009BSB09800).

References

[1] J.T. Spadary, L. Isebelle, V. Renganathan, Hydroxyl radical mediated degradation of azo dyes: evidence for benzene generation, Environ. Sci. Technol. 28 (1994) 1389–1393.
[2] K.T. Chung, G.E. Fulk, A.W. Andres, Mutagenicity testing of some commonly used dyes, Appl. Environ. Microbiol. 42 (1981) 641–648.
[3] H.Y. Shu, W.P. Hsieh, Treatment of dye manufacturing plant effluent using an annular UV/H_2O_2 reactor with multi-UV lamps, Sep. Purif. Technol. 51 (2006) 379–386.
[4] S.F. Kang, C.H. Liao, S.T. Po, Decolorization of textile wastewater by photo-Fenton oxidation technology, Chemosphere 41 (2000) 1287–1294.
[5] M.S. Lucas, J.A. Peres, Decolorization of the azo dye Reactive Black 5 by Fenton and photo-Fenton oxidation, Dyes Pigments 71 (2006) 236–244.
[6] A.B. dos Santos, F.J. Cervantes, J.B. van Lier, Review paper on current technologies for decolourisation of textile wastewaters: perspectives for anaerobic biotechnology, Bioresour. Technol. 98 (2007) 2369–2385.

[7] M. Kornaros, G. Lyberatos, Biological treatment of wastewaters from a dye manufacturing company using a trickling filter, J. Hazard. Mater. 136 (2006) 95–102.
[8] Y. Fu, T. Viraraghavan, Fungal decolorization of dye wastewaters: a review, Bioresour. Technol. 79 (2001) 251–262.
[9] J. Gao, Q. Zhang, K. Su, R. Chen, Y. Peng, Biosorption of Acid Yellow 17 from aqueous solution by non-living aerobic granular sludge, J. Hazard. Mater. 174 (2010) 215–225.
[10] S. Aber, N. Daneshvar, S.M. Soroureddin, A. Chabok, K. Asadpour-Zeynali, Study of acid orange 7 removal from aqueous solutions by powdered activated carbon and modelling of experimental results by artificial neural network, Desalination 211 (2007) 87–95.
[11] B.H. Hameed, I.A.W. Tan, A.L. Ahmad, Optimization of basic dye removal by oil palm fibre-based activated carbon using response surface methodology, J. Hazard. Mater. 158 (2008) 324–332.
[12] I.A.W. Tan, A.L. Ahmad, B.H. Hameed, Adsorption of basic dye using activated carbon prepared from oil palm shell: batch and fixed bed studies, Desalination 225 (2008) 13–28.
[13] B.H. Hameed, A.T.M. Din, A.L. Ahmad, Adsorption of methylene blue onto bamboo-based activated carbon: kinetics and equilibrium studies, J. Hazard. Mater. 141 (2007) 819–825.
[14] B.H. Hameed, A.L. Ahmad, K.N.A. Latiff, Adsorption of basic dye (methylene blue) onto activated carbon prepared from rattan sawdust, Dyes Pigments 75 (2007) 143–149.
[15] M. Hadi, M.R. Samarghandi, G. McKay, Equilibrium two-parameter isotherms of acid dyes sorption by activated carbons: study of residual errors, Chem. Eng. J. 160 (2010) 408–416.
[16] L.S. Chan, W.H. Cheung, S.J. Allen, G. McKay, Separation of acid-dyes mixture by bamboo derived active carbon, Sep. Purif. Technol. 67 (2009) 166–172.
[17] S. Karcher, A. Kornmüller, M. Jekel, Screening of commercial sorbents for the removal of reactive dyes, Dyes Pigments 51 (2001) 111–125.
[18] S. Karcher, A. Kornmüller, M. Jekel, Anion exchange resins for the removal of reactive dyes from textile wastewaters, Water Res. 36 (2002) 4717–4724.
[19] M. Wawrzkiewicz, Z. Hubicki, Removal of tartrazine from aqueous solutions by strongly basic polystyrene anion exchange resins, J. Hazard. Mater. 164 (2009) 502–509.
[20] M. Wawrzkiewicz, Z. Hubicki, Equilibrium and kinetic studies on the sorption of acidic dye by macro porous anion exchange, Chem. Eng. J. 157 (2010) 29–34.
[21] H. Yoshida, A. Okamoto, T. Kataoka, Adsorption of acid dye on cross-linked chitosan fibers-equilibria, Chem. Eng. Sci. 48 (1993) 2267–2272.
[22] V. Singh, A.K. Sharmaa, R. Sanghi, Poly(acrylamide) functionalized chitosan: an efficient adsorbent for azo dyes from aqueous solutions, J. Hazard. Mater. 166 (2009) 327–335.
[23] P.K. Malik, Use of activated carbons prepared form sawdust and rice-husk for adsorption of acid dyes: a case study of Acid Yellow 36, Dyes Pigments 56 (2003) 239–249.
[24] A.A. Attia, W.E. Rashwan, S.A. Khedr, Capacity of activated carbon in the removal of acid dyes subsequent to its thermal treatment, Dyes Pigments 69 (2006) 128–136.
[25] M. Wawrzkiewicz, Z. Hubicki, Equilibrium and kinetic studies on the sorption of acidic dye by macroporous anion exchanger, Chem. Eng. J. 157 (2010) 29–34.
[26] Y.C. Wong, Y.S. Szeto, W.H. Cheung, G. McKay, Adsorption of acid dyes on chitosan-equilibrium isotherm analyses, Process Biochem 39 (2004) 693–702.
[27] C. Shen, S. Song, L. Zang, X. Kang, Y. Wen, W. Liu, L. Fu, Efficient removal of dyes in water using chitosan microsphere supported cobalt (II) tetrasulfophthalocyanine with H_2O_2, J. Hazard. Mater. 177 (2010) 560–566.
[28] J. Yin, Z. Meng, M. Du, C. Liu, M. Song, H. Wang, Pseudo-template molecularly imprinted polymer for selective screening of trace β-lactam antibiotics in river and tap water, J. Chromatogr. A 1217 (2010) 5420–5426.
[29] H.S. Byun, Y.N. Youn, Y.H. Yunc, S.D. Yoon, Selective separation of aspirin using molecularly imprinted polymers, Sep. Purif. Technol. 74 (2010) 144–153.
[30] Y. Sueyoshi, C. Fukushima, M. Yoshikawa, Molecularly imprinted nanofiber membranes from cellulose acetate aimed for chiral separation, J. Membr. Sci. 357 (2010) 90–97.
[31] P. Chang, Z. Zhang, C. Yang, Molecularly imprinted polymer-based chemiluminescence array sensor for the detection of proline, Anal. Chim. Acta 666 (2010) 70–75.
[32] M. Tada, Y. Iwasawa, Design of molecular-imprinting metal-complex catalysts, J. Mol. Catal. A: Chem. 199 (2003) 115–137.
[33] M. Le Noir, B. Guieysse, B. Mattiasson, Removal of trace contaminants using molecularly imprinted polymers, Water Sci. Technol. 53 (2006) 205–212.
[34] M. Le Noir, A.-S. Lepeuple, B. Guieysse, B. Mattiasson, Selective removal of 17[beta]-estradiol at trace concentration using a molecularly imprinted polymer, Water Res. 41 (2007) 2825–2831.
[35] M. LeNoir, P. Plieva, T. Hey, B. Guieysse, B. Mattiasson, Macro porous molecularly imprinted polymer/cryogel composite systems for the removal of endocrine disrupting trace contaminants, J. Chromatogr. A 1154 (2007) 158–164.
[36] Z. Meng, W. Chen, A. Mulchandani, Removal of estrogenic pollutants from contaminated water using molecularly imprinted polymers, Environ. Sci. Technol. 39 (2005) 8958–8962.
[37] Y. Li, X. Li, J. Chu, C. Dong, Synthesis of core–shell magnetic molecular imprinted polymer by the surface RAFT polymerization for the fast and selective removal of endocrine disrupting chemicals from aqueous solutions, Environ. Pollut. 158 (2010) 2317–2323.
[38] J. Pan, X. Xue, J. Wang, H. Xie, Z. Wu, Recognition property and preparation of Staphylococcus aureus protein A-imprinted polyacrylamide polymers by inverse-phase suspension and bulk polymerization, Polymer 50 (2009) 2365–2372.
[39] C. Michailof, P. Manesiotis, C. Panayiotou, Synthesis of caffeic acid and p-hydroxybenzoic acid molecularly imprinted polymers and their application for the selective extraction of polyphenols from olive mill waste waters, J. Chromatogr. A 1182 (2008) 25–33.
[40] H. Sun, F. Qiao, Recognition mechanism of water-compatible molecularly imprinted solid-phase extraction and determination of nine quinolones in urine by high performance, J. Chromatogr. A 1212 (2008) 1–9.
[41] Y. Zhang, R. Liu, Y. Hu, G. Li, Microwave heating in preparation of mag-MIP beads for trace triazines analysis in complicated sample, Anal. Chem. 81 (2009) 967–976.
[42] C.J. Tan, H.G. Chua, K.H. Ker, Y.W. Tong, Preparation of bovine serum albumin surface-imprinted submicrometer particles with magnetic susceptibility through core–shell miniemulsion polymerization, Anal. Chem. 80 (2008) 683–692.
[43] L.M.C. Antonio, M. Günter, F.F.S. Jorge, S.C. Antonio, K. Ingo, F.G. Alberto, Novel strategy to design magnetic, molecular imprinted polymers with well-controlled structure for the application in optical sensors, Macromolecules 43 (2010) 55–61.
[44] E Corton, J.A. García-Calzón, M.E. Díaz-García, Kinetics and binding properties of cloramphenicol imprinted polymers, J. Non-Cryst. Solids 353 (2007) 974–980.
[45] J.A. García-Calzón, M.E. Díaz-García, Characterization of binding sites in molecularly imprinted polymers, Sens. Actuator B 123 (2007) 1180–1194.
[46] Y.S. Ho, G. McKay, Kinetic models for the sorption of dye from aqueous solution by wood, Trans. Inst. Chem. Eng. 76B (1998) 183–191.